Check for updates

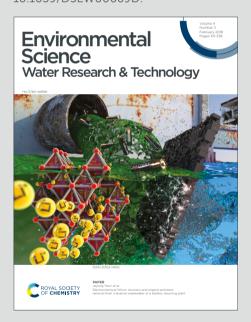
Environmental Science



Water Research & Technology

Accepted Manuscript

This article can be cited before page numbers have been issued, to do this please use: W. Tomaszewski, K. Andrzej, M. Zybert, P. Wieciski and G. Tomasz, *Environ. Sci.: Water Res. Technol.*, 2025, DOI: 10.1039/D5EW00669D.



This is an Accepted Manuscript, which has been through the Royal Society of Chemistry peer review process and has been accepted for publication.

Accepted Manuscripts are published online shortly after acceptance, before technical editing, formatting and proof reading. Using this free service, authors can make their results available to the community, in citable form, before we publish the edited article. We will replace this Accepted Manuscript with the edited and formatted Advance Article as soon as it is available.

You can find more information about Accepted Manuscripts in the <u>Information for Authors</u>.

Please note that technical editing may introduce minor changes to the text and/or graphics, which may alter content. The journal's standard <u>Terms & Conditions</u> and the <u>Ethical guidelines</u> still apply. In no event shall the Royal Society of Chemistry be held responsible for any errors or omissions in this Accepted Manuscript or any consequences arising from the use of any information it contains.



Open Access Article. Published on 29 July 2025. Downloaded on 8/11/2025 11:18:36 AM.

This article is licensed under a Creative Commons Attribution 3.0 Unported Licence.

Water impact View Article Online DOI: 10.1039/D5EW00669D

Explosives are classified as emerging contaminants in recent years. A novel adsorbent was prepared from waste polycarbonate and cotton fabric, for the removal of nitro explosives from water. In laboratory and bench scale the adsorbent is characterized by high adsorption capacity.

- 1 Efficient preparation of adsorption beds from polycarbonate and View Article Online Online
- 2 cotton fabric wastes: Removal of nitroaromatic pollutants from water
- 4 Tomaszewski Waldemar ^{a *}, Krasiński Andrzej ^b, Zybert Magdalena ^a, Wieciński Piotr ^a,
- 5 Gołofit Tomasz ^a

6

- 7 The pollution of the environment with explosives and their decomposition products,
- 8 particularly resulting from armed conflicts and intensive mining activities, poses a serious
- 9 problem nowadays. In this work, the properties of novel and environmentally neutral
- 10 adsorbent were investigated, which was used further to remove nitroaromatic explosives from
- 11 wastewater. The adsorbent was prepared in a straightforward way from waste raw materials
- by applying a composite of polycarbonate and fumed silica to cotton fabric. On both
- 13 laboratory and bench scale (flow system with recirculation), a new bed demonstrated high
- efficiency for removal of nitroaromatics from water, exceeding 90% for trinitrotoluene
- 15 (TNT). It was also confirmed that the bed is suitable for removing explosive substances from
- the real river water. The sorption properties of the material were related to its characteristics
- obtained using spectroscopic, microscopic, and thermal analysis, nitrogen adsorption, as well
- as adsorption kinetics and isotherms.
- 20 a Warsaw University of Technology, Faculty of Chemistry, 3 Noakowskiego Street, 00-664
- 21 Warsaw, Poland;

19

- 22 b Warsaw University of Technology, Faculty of Chemical and Process Engineering,
- Waryńskiego 1 Street, 00-645 Warsaw, Poland.

[†] Electronic supplementary information (ESI) available.

View Article Online DOI: 10.1039/D5EW00669D

- * Corresponding author
- 27 E-mail address: waldemar.tomaszewski@pw.edu.pl (W. Tomaszewski),
- 28 <u>https://orcid.org/0000-0002-2275-2479</u>

1. Introduction

from two significant categories of anthropogenic waste - namely, waste textiles and waste plastics, specifically cotton fabric and polycarbonate - for the removal of hazardous environmental toxins, particularly nitroaromatic compounds, from aqueous solutions. The first section of the introduction provides a brief overview of the selected waste materials and the environmental risks associated with nitro compounds. These two issues are then brought together in the final part of the introduction, forming the conceptual basis of the paper.

Textile and plastics production constitute important sectors of the global economy, with millions of employees worldwide. The global production and disposal of textiles composed of both natural-origin materials and fibrillated polymers, along with a variety of plastic products exhibiting diverse morphologies, is constantly growing. This trend presents significant environmental and societal challenges. This requires a comprehensive global framework for the management, disposal, and environmental monitoring of such materials, particularly in natural systems such as aquatic environments, soils, and even the atmosphere, where fragmented forms, most notably microplastics, may accumulate and persist.

This study presents a novel approach for the simultaneous utilization of materials derived

- In 2022 the global textile production amounted to 116 million of tones ¹, whereas the View Article Online Online
- 47 production of plastics 400 millions of tons ².
- 48 Both production types experienced a significant growth compared to 2021. The two industries
- 49 have been criticized for unsustainable use of water, land, fossil fuels and energy, as well as
- 50 production processes involving toxic chemicals, waste and pollution. Currently, millions of
- 51 tons of waste such as used clothes and plastics raise a major concern as well, and therefore
- more attempts to recycle textiles ³ and plastics ⁴ are undertaken. The works on the use of
- waste textiles and plastics to remove other environmental pollutants have been published.
- Fabric-based adsorbents have been used to remove various pollutants from water, including
- pesticides 5, heavy metals 6 and dyes 7. There have also been attempts to use plastic waste to
- produce adsorbents that would eliminate heavy metals ⁸, oil stains ⁹ and dyes ¹⁰ from water.
- Nitroaromatic compounds represent a group of hazardous environmental pollutants that are
- 58 neurotoxic and are possible human carcinogens ¹¹. Due to their high chemical stability and
- persistence, these compounds can remain in water and soil for extended periods of time ¹².
- 60 This group of compounds primarily includes components of explosives that enter the
- environment as a result of military, mining, and armament production activities. In addition to
- such activities, these compounds are also used in chemical processing, for example,
- dinitrotoluenes are used in the production of polyurethanes ¹³. Significant environmental
- 64 contamination by nitrotoluenes also occurs as a result of armed conflicts (e.g., in Syria,
- 65 Ukraine, and Central Africa) ¹⁴.
- Technologies for removing nitrotoluenes from the aquatic environment are primarily based on
- 67 separation methods and degradation processes ¹⁵. Among separation methods, adsorption is
- the most commonly used ¹⁶. For the degradation of nitroaromatics, commonly employed

72

73

74

75

76

77

78

79

80

81

82

83

84

85

86

87

88

89

90

91

92

methods include advanced oxidation processes (AOPs), such as the Photo–Fenton process of the Photo–Fenton process

Among these remediation techniques, adsorption on granular activated carbon (GAC) is most frequently applied for treating surface waters. This is due to the simplicity and effectiveness of the method. However, it comes with high costs related to GAC production, disposal of spent carbon, or its regeneration ¹⁵. It should be noted that high-temperature carbon regeneration is not used due to safety risks when the explosive content in the matrix exceeds 8% by weight ²⁰. Other methods such as hydrolysis ²¹, solvent extraction ²², or heat steam–air treatment ²³ are used for regenerating activated carbon loaded with explosives. However, the high energy and chemical consumption involved in these processes drive the search for more sustainable and cost-effective adsorbents for the removal of nitroaromatics from surface waters. Recent studies suggest that adsorbents derived from agricultural or industrial waste may offer promising and economical alternatives. For instance, activated carbon obtained from spent coffee grounds has been shown to have low production costs and allows for easy solvent regeneration after TNT adsorption ²⁴. Another inspiration for the below study came from a paper published in 2018 ²⁵. This work used thin film passive samplers prepared on various substrate materials, including cotton,

coated by dip-coating in solutions of polymers based on 2,6-diphenylene oxide, such as Tenax TA or PPO. The prepared samplers demonstrated efficient adsorption capacity of nitroaromatic vapors of explosive substances. The above results, along with a earlier publication ²⁶ on the adsorption of explosives on acrylic and aromatic polymers, inspired the idea of preparing polycarbonate-based adsorption media for the removal of nitroaromatic compounds from water. In line with the above, the authors of this study aimed to explore the use of post-consumer waste, specifically cotton fabrics waste and offcuts of polycarbonate

96

97

98

99

100

101

102

103

104

105

106

107

108

109

110

111

112

113

114

115

116

sheets, for the development of a novel sustainable 27 adsorbent. To date, no published studies Article Online Sheets and a novel sustainable 27 adsorbent. To date, no published studies Article Online Sheets and Sheets are supported by the studies of the development of a novel sustainable 27 adsorbent. To date, no published studies are supported by the studies of the development of a novel sustainable 27 adsorbent. To date, no published studies are supported by the studies of the development of a novel sustainable 27 adsorbent. To date, no published studies are supported by the studies of the studies 93 94

have reported such a use of these waste materials.

2. Materials and methods

2.1. Waste raw materials and chemicals

The polycarbonate (PC) came from the waste from panels used by a local canopy manufacturer. The 5 mm thick, triangle shaped waste (Fig. S1 in the Supplementary Material) was cut into smaller pieces using a hand-held metal guillotine. The cotton substrate came from unused 140 g/m² cotton fabric withdrawn from military warehouse (Figure S2). As a solvent waste tetrahydrofuran (THF) was used. It source was an effluent from the analysis by size exclusion chromatography (SEC), originally being an unstabilized BHT solvent of chromatographic purity (Avantor, Poland). Silica gel – analyzed sorbent for flash chromatography (irregular 40 - 63 µm, 60 Å) was obtained from Baker (Poland), whereas Aerosil R 972 V was obtained from Evonik. Aerosil R 972 V is a densified hydrophobic fumed silica, after being treated with dimethyldichlorosilane. Norit SX-2 activated carbon was obtained from Chempur (Poland). Acetonitrile for liquid chromatography and deionized water were used for high performance liquid chromatography (HPLC) quantification of explosives, while the substances: 2,4,6-trinitrotoluene (TNT), 2,4-dinitrotoluene (2,4-DNT), 1,3,5-trinitrobenzene (TNB), 2-nitrotoluene (2-NT), 1-nitronaphthalene (1-NN), 1,8dinitronataphthalene (1,8-DNN) came from the Department of Chemistry, Warsaw University of Technology.

2.2. Preparation and properties of adsorption bed

2.2.1. Adsorption bed preparation

Adsorption beds were obtained by applying a solution of PC in THF, with or without silica, to both sides of the cotton fabric using a paint roller with cotton coating. After the bed

118

119

120

121

122

123

124

125

126

127

128

129

130

131

132

133

134

composition had been optimized (see discussion point 2.2.2.2.), a solution in 720 ml of THE Article Online with 23 g of PC and 25 g of silica or Aerosil was used to prepare the adsorption beds. A metal frame, to which a 28 x 58 cm fabric (Figure S3) was attached, was placed under the ventilation hood. Each side of the central area of the 20 x 50 cm fabric was progressively and evenly covered with half of the solution, using transverse and longitudinal movements of the roller. A total of 10-11 such cycles were completed, and after application of the phase, THF needed some time to evaporate. The fabric was then removed from the frame and fixed again with reverse side. The bed was left to dry overnight and then cut into appropriate size (Fig. 1). The reference material, i.e. containing only PC was prepared in a similar way. The beds prepared on cotton fabric (C) were marked as follows: reference PC/C, with silica PC/Si/C, and with Aerosil PC/Ae/C. For differential scanning calorimetry (DSC) and scanning electron microscopy (SEM) measurements, the samples of the adsorption phase alone were prepared, i.e. the one not applied to the cotton, but poured to form thin layers in Petri dishes. In the case of DSC, this was caused by the fact that the decomposition of the cotton begins at temperatures above 180°C. For SEM, this step facilitated the measurements and, most importantly, allowed the observation of undamaged samples. The obtained samples were designated as PC/THF,

- 135 Fig. 1
- 136 2.2.2. Bed characteristics
- 137 2.2.2.1. Efficient amount of phase on textile

PC/Si, and PC/Ae, respectively.

In order to determine the mass of applied phase, a central part i.e. 20 x 50 cm was cut out from each bed and weighed. The mass of the fabric, i.e. 14 g was subtracted from resulting weight.

View Article Online

DOI: 10.1039/D5EW00669D

142

143

145

146

147

148

149

150

151

152

153

154

155

156

157

158

160

161

162

163

164

141 2.2.2.2. Fourier transform infrared spectroscopy (FTIR)

FTIR measurements were performed to determine the extent of coverage of the fabric by the applied phase. FTIR spectra were collected on Nicolet 6700 spectrometer (Thermo Scientific)

using an ATR accessory. Thirty two scans were taken at a resolution of 4 cm⁻¹ each.

2.2.2.3. Raman spectroscopy

The Raman spectra of prepared cotton beds were collected to determine the crystal/disordered structure of PC. For this purpose the intensities of the bands obtained from the deconvoluted spectra in the 750–710 and 1275–1200 cm⁻¹ regions were compared. The spectra were recorded using Thermo Nicolet Almega XR Raman spectrometer (Thermo Electron). Excitation was achieved using a 532 nm laser. The deconvolution of the bands was carried out using Omnic software (Thermo Fisher v. 9.1).

2.2.2.4. Low-temperature nitrogen adsorption

N₂ physisorption was applied to determine the specific surface area and total pore volume of the studied materials. The experiments were conducted at –196 °C using an ASAP2020 instrument (Micromeritics Instrument). Before the measurements, each sample was subjected to a two-step degassing procedure in vacuum: at 90 °C for 1h and then at 120 °C for 4h. The obtained data were approximated using Brunauer-Emmett-Teller (BET) and Barret-Joyner-Halenda (BJH) isotherm models.

159 2.2.2.5. Scanning electron microscopy (SEM)

Morphology and microstructure observation, as well as chemical analysis, were performed with the use of field emission scanning electron microscope Helios 5 PFIB (Thermo Scientific) equipped with Xe plasma FIB column and EDS spectrometer Octane Elice (EDAX). Thin Au coating was deposited onto the samples in order to ensure the conductivity of the surface. SE signal was applied to observe the surface morphology of the material.

165 2.2.2.6. Differential scanning calorimetry (DSC)

View Article Online DOI: 10.1039/D5EW00669D

In order to compare the degree of crystallinity of prepared adsorbents DSC studies were performed, using a DSC Q2000 differential scanning calorimeter (TA Instruments). Indium was used for calibration as a standard substance. Measurements were carried out in open pans at temperatures from -100 to 300 °C, with a constant temperature increase of 10 °C/min and nitrogen flow of 50 mL s $^{-1}$.

2.2.2.7. UV-Vis spectrophotometry

UV-Vis absorption spectra of real river water samples were recorded on a Evolution 60S spectrophotometer (Thermo Scientific) at room temperature. Redistilled water was used as a reference sample.

2.3. Bed adsorption

2.3.1. Laboratory scale

The adsorption (q_t) of nitroaromatic substances from aqueous solutions on the prepared beds was expressed as the amount of substance adsorbed after fixed time (t) per mass unit of used bed and was calculated according to the formula:

$$q_t = \frac{(C_0 - C_t)}{m} V \tag{1}$$

where: q_t - amount of substance adsorbed after time t (mg/g), C_o - initial concentration (mg/L), C_t - concentration after time t (mg/L), V – solution volume (L), m – bed mass (g). The adsorption kinetics was examined on two scales: lab-scale (1 liter) and bench scale (16 liters). On the lab-scale, 1 liter of nitro compound solutions with a concentration of 25 mg/L in redistilled water was placed in a 2 liter beaker. Such high concentration levels were chosen to ensure the collection of accurate and reproducible analytical data also in the case when high level of the analyte has been removed by the beds. An adsorption bed in form of 60 pieces –

189

190

191

192

193

194

195

196

197

198

199

200

201

202

203

204

205

206

207

208

209

210

211

212

flakes of 1 x 1 cm was added to the beaker. The solutions were mixed at room temperature at room temperature online using a mechanical turbine stirrer at 200 rpm. Samples were collected at different time intervals depending on the experimental stage and analyzed by HPLC as described below. Such experimental setup for the lab-scale was chosen based on preliminary studies performed for TNT, where the variable parameters involved the rotation of stirrer and ionic strength of the solutions. The rotation was changed in the range of 0 - 400 rpm, while the ionic strength was increased using the addition of NaCl, i.e. 1% and 5%. On the other hand, the adsorption isotherms were determined for TNT only. This relates to the conclusions in the discussion below, namely that the adsorption kinetics of the investigated nitro compounds show great similarities. Experiments to determine TNT adsorption isotherms on PC/Si/C and PC/Ae/C beds were performed on a scale proportional to the kinetic experiments, i.e. a 30-times reduced scale. 33 mL of aqueous solutions with concentrations ranging from 0.25 to 25 mg/L and two flakes of the size 1 x 1 cm were added to 50 mL conical glass flasks with screw caps. The flasks were shaken at 26 °C, 36 °C, and 46 °C, for 24 hours. The collected samples were analyzed by HPLC as described below (point **2.3.3.**). In order to determine the effect of the natural matrix on the sorption capacity of the Pc/Ae/C adsorbent, the experiments were carried out on a 1-litre scale using flowing water from the Pilica River near Białobrzegi town, central Poland. After sedimentation, the water was poured into 1-liter volumetric flasks and stored in a refrigerator. Before starting the experiments, the contents of the flasks was poured into 2-litre beakers, where 1 ml of acetonitrile containing 25 mg of the nitro compound was added. According to previous work ²⁸ the addition of acetonitrile eliminated the biological activity in the water (bacteria, fungi) and stabilized its properties. After mixing the solutions, the corresponding samples were taken. Then the experiments were carried out as in case of lab-scale, except that only 3 samples were taken from each beaker after 48 hours of the experiment. The samples were filtered through 0.45

μm PTFE filters. HPLC analyses served to determine concentrations and calculate the bed rew Article Online
 adsorption values designated as q_{river} (river) for investigated nitroaromatics.

2.3.2 Bench scale

Experiments of sorption were carried out in the system, which can be operated continuously in a wide range of flow rates (high flexibility), and can be easily scaled up to a desired capacity. Presented results show the performance of water cleaning in a closed loop, in which the liquid was circulated from the tank through the column containing sorbent elements. The system layout is schematically shown on the process flow diagram in Figure 2.

Figure 2.

Around 16 liters of water solution of a pollutant was prepared and poured into the tank (1) before each experiment. The initial concentration was 25 mg/L. Then the circulation pump (2) (centrifugal, produced by Grundfos, model CRNE 1-3) was switched on and the process was initiated. The water was pumped from the tank (1) through the vertical glass column and returned to the feed tank. The flow rate was controlled using the mass flow meter (3) (manufactured by Endress+Hauser, model Promass 40E15) and manually adjusted using the diaphragm valve (4); flow rate 400 L/h was used in experiments. The water samples for analysis were collected every 15 minutes (first hour) and next every 30 minutes. During the experiment the pressure drop on the column was also monitored. The flow characteristics of the experimental system is shown in Fig. S4. The column ID was 15 cm, and the total length 40 cm. The sorbent elements – 1000 flakes of 1 x 1 cm were loosely packed on perforated plate (5 mm holes, free area around 30%) made of polyethylene.

2.3.3. Quantification of nitroaromatics in solutions

The aqueous solutions of nitro compounds – samples before and after experiments – were analysed using high-performance liquid chromatography (HPLC) using an Agilent 1260 Infinity system with UV DAD detector. The separation was carried out with mobile phase

- acetonitrile/water on Supelcosil ABZ+ column 150 mm × 4.6 mm at 50 °C. HPLC grade View Article Online View Article Online Online View Article Online Online View Article Online View Artic
- solvents were used. The taken aqueous samples were analysed without any preparation.
- 240 2.3.4. Adsorption kinetics analysis of data
- 241 Two kinetic equations have been used to describe the mechanism of adsorption kinetic data: a
- 242 pseudo-first-order and a pseudo-second-order equation. The pseudo-first order equation ²⁹ has
- 243 the following linear form:

$$ln(q_e - q_t) = q_e ln - \left(\frac{k_1}{2.303}\right)$$
 (2)

- 245 where: q_e amount of adsorption at equilibrium (mg/g), q_t amounts of adsorption at time t
- 246 (mg/g), k_I first-order equation constant (1/min), t time (min).
- 247 The linear form of the pseudo-second-order equation ³⁰ is as follows:

$$\frac{t}{q_t} = \frac{1}{k_2 \, q_e^2} + \frac{t}{q_e} \tag{3}$$

- where: q_t amounts of adsorption at time t (mg/g), q_e –amount of adsorption at equilibrium
- 250 (mg/g), k_2 second-order equation constant (g/(mg·min)), t time (min).
- 251 2.3.5. Absorption isotherm data analysis
- 252 Two adsorption isotherm equations were used to describe the adsorption of nitro compounds,
- 253 namely Langmuir and Freundlich models.
- 254 The linear form of Langmuir isotherm model ³¹ is as follows:

$$\frac{C_e}{q_e} = \frac{C_e}{q_m} + \frac{1}{K_L q_m} \tag{4}$$

- where: C_e concentration of solution at equilibrium (mg/L), q_e amount of adsorbed nitro
- 257 compound at equilibrium (mg/g), q_m maximum adsorption capacity (mg/g), K_L Langmuir
- 258 constant (L/mg).

259 The linear form of Freundlich isotherm equation ³¹ is as follows:

View Article Online DOI: 10.1039/D5EW00669D

$$log q_e = \left(\frac{1}{n}\right) log C_e + log K_F \tag{5}$$

- where: q_e amount of adsorbed nitro compound at equilibrium (mg/g), n constant, C_e –
- 262 concentration of solution at equilibrium (mg/L), K_F Freundlich constant (mg/g).
- 263 2.3.6. Adsorption thermodynamics data analysis
- The thermodynamic parameters of adsorption, i.e., free energy change (ΔG), change in enthalpy (ΔH), and change in entropy (ΔS), determine the spontaneity and feasibility of the adsorption process, as well as the influence of temperature on its course. The determination of
- thermodynamic parameters is based on the van't Hoff equation, which is expressed as
- 268 follows:

This article is licensed under a Creative Commons Attribution 3.0 Unported Licence.

Open Access Article. Published on 29 July 2025. Downloaded on 8/11/2025 11:18:36 AM.

$$lnK_{eq} = -\frac{\Delta H}{RT} + \frac{\Delta S}{R} \qquad (6)$$

- where R is the universal gas constant (8.314 J/mol/K), T is the temperature (K), and K_{eq} is the equilibrium constant. A plot of lnK_{eq} versus 1/T allows for the determination of ΔH and ΔS as the slope and intercept of the linear plot, respectively, multiplied by R.
- 273 The value of ΔG can be calculated using the equation:

$$\Delta G = -RT ln K_{eq} = \Delta H - T \Delta S \tag{7}$$

- For the non-ionic analyte studied, e.g. TNT (trinitrotoluene), the dimensionless equilibrium
- 276 constant K_{eq} was obtained from the Langmuir constant K_L , according to Ghosal and Gupta 32 ,
- by multiplying K_L by the molar mass of TNT expressed in mg/mol (227.13 10^3).

278

View Article Online

DOI: 10.1039/D5EW00669D

280

281

282

283

284

285

286

287

288

289

290

291

292

293

294

295

296

297

298

299

300

301

302

303

2.3.7. Solvent desorption studies

To investigate the desorption efficiency of TNT from PC/Ae/C, three samples of the sorbent with a known amount of deposited TNT were prepared. The samples were prepared in the same way as for the determination of adsorption isotherms. 33 mL of aqueous TNT solutions at a concentration of 25 mg/L and two flakes (1 × 1 cm in size) were placed in 50 mL conical glass flasks with screw caps. The flasks were shaken at 26 °C for 24 hours. After this time, the aqueous phases were collected and analyzed by HPLC. The equilibrium concentrations of TNT allowed the calculation of the amount of TNT adsorbed onto the sorbent. The pre-adsorbed samples were subjected to extraction with acetonitrile (ACN). ACN was chosen because it is a good solvent for TNT and does not dissolve polycarbonate. Furthermore, the resulting extract can be directly analyzed by the applied HPLC method, unlike, for example, an acetone extract, which must be evaporated to dryness and then reconstituted before analysis. The desorption of TNT was carried out as follows. After the experiments, the sorbent samples were rinsed with water and dried on filter paper. Desorption was performed in 4 mL screw-cap vials containing two pieces of the sorbent, 2 mL of ACN, and a magnetic stir bar. The extraction was conducted for 15 minutes. Prior to analysis, the extract was diluted 16.5-fold with water (the initial volume of water sample was 33 mL).

3. Results and discussion

3.1 Adsorbent preparation

In preparation of 10 consecutive beds, it was found that the application of an average of 36 mg \pm 1 mg of PC/Aerosil adsorbent phase and 33 mg \pm 1 mg of PC/silica adsorbent phase per 1 cm² of fabric was possible. These values should be understood as the total amount of adsorbent present on both sides of the fabric. It should be recalled that based on the bed preparation conditions the maximum coverage could be 48 mg per 1 cm².

305

306

View Article Online

DOI: 10.1039/D5EW00669D

307 308 309 310 311 312 313 314 315

This article is licensed under a Creative Commons Attribution 3.0 Unported Licence.

316

317

318

319

320

321

323

324

325

326

327

Open Access Article. Published on 29 July 2025. Downloaded on 8/11/2025 11:18:36 AM.

3.2. FTIR spectroscopy

Fig. 3 shows the spectra of reagents used to prepare beds, as seen from top to bottom: Aerosil (A), cotton fabric (B), polycarbonate (C), fabric of coverage of 30 mg / cm² of the PC + Aerosil mixture (D), and of 36 mg / cm² coverage (E). The most intense observed vibrations are discussed below. For Aerosil the peak at 1100 cm⁻¹ (marked 1) can be attributed to asymmetric stretching vibrations of the Si-O-Si bonds and the peak at 820 cm⁻¹ (2) can be assigned to the symmetric deformation vibration of the Si-O-Si bonds. For cotton fabric broad band 3300 cm⁻¹ (3) represent O-H stretching vibration and at 1030 cm⁻¹ (4) C-O stretching vibration. For polycarbonate the characteristic peaks can be assigned as follows: at 1770 cm⁻¹ (5) C=O stretching vibration, 1500 cm⁻¹ (6) aromatic C-C stretching and 1230 – 1200 cm⁻¹ (6) three peaks for O-C-O asymmetric stretching. The spectrum of cotton with a coverage of 30 mg / cm² of the PC/Aerosil mixture is still characterized by O-H and C-O vibrations in cotton and PC vibration is also clearly visible. The broad bands of low specificity for silica are not represented. The O-H (3) and C-O (4) vibrations are no longer visible on the spectrum of

cotton with a coverage of 36 mg/cm², while the broad bands attributed to Aerosil (1 and 2)

can be observed. In comparison to the spectrum above (D in Fig. 3), the intensity of the bands

attributed to PC is higher. Therefore, for the coverage of cotton with the phase at the value of

36 mg/cm², it was considered that the surface is completely covered by the adsorbent.

322 Figure 3.

3.3. Raman spectroscopy

The Raman spectroscopy was previously reported as a useful tool for analysis of the crystal structures of PC ³³. In accordance with this work the degree of the ordered structure of the PC can be estimated from the intensity ratio of the peak at 727 cm⁻¹ (order band) and 735 cm⁻¹ (disorder band), and also the intensity ratio of the peak at 1248 cm⁻¹ (order band) and

1235 cm⁻¹ (disorder band). In short, the higher the intensity ratio, i.e. I_{727}/I_{735} and $I_{D248}/I_{D328}/I_$

Table 1.

It was recently shown that the ordered – crystalline structure of PC formed after the evaporation of its solution in THF strongly interacts with the surface of carbon fibres through π - π interactions of phenyl rings ³⁴. It can be assumed that such interactions also occur during the adsorption of nitroaromatic substances on prepared substrates. The increase in the adsorption of trinitrotoluene (TNT) for successive PC/C – PC/Si/C – PC/Ae/C substrates (see Figure 6) can be correlated with the increase in crystallinity of these substrates as per Raman measurements (see Table 1). Finally, it should be added that in the reviewed literature on PC composites, no reports were found regarding the impact of inorganic particles added to them on the crystallinity of the composites.

3.4. Low temperature nitrogen adsorption

The textural features of the studied materials (Table 2) show clear differences depending on the material composition. The S_{BET} of the samples of cotton and PC/C is very low (below 1 m²/g). After introducing of additional component (Aerosil R972V or silica) to prepared materials, the S_{BET} significantly increased. The highest S_{BET} 72.9 m²/g is observed for the material containing silica (PC/Si/C).

350 Table 2.

Figure S6 presents the N₂ adsorption-desorption isotherms, which according to the ILIPACCE OF DIAGNOSCIED CLASSIFICATION OF SERVICE CONTINUES AND ACCESSIFICATION OF THE CONTINUES AND ACCESSIFICA

3.5. SEM analysis

At 200x magnification (Fig. 4), the surfaces of PC/THF and PC/Ae samples are smooth except for mechanical damage. The PC/Si sample shows quite evenly distributed silica particles surrounded by a smooth polycarbonate matrix. At a higher magnification of 35.000x, the PC/THF surface appears smooth, although some cracks can be observed at that stage. In contrast, the surface of the polymer in PC/Si changes; it is rough and irregular areas of different textures can be found. They appear as extended clusters of polymer phase of different densities, or, alternatively, as the structures grouped into bundles or cylinders ³⁶. At corresponding magnification, the PC/Ae surface is uneven, with numerous holes, gaps and clusters of smaller, oval particles.

At an even higher magnification of 100.000x, narrow 50-100 nm long cracks can be observed

on the smooth PC/THF surface. The PC/Si surface is more extensively cracked than the

PC/THF, with many more, however wider cracks of similar length. At the highest view Article Online magnification the PC/Ae surface is well developed and irregular, oval holes, pores measuring 50-200 nm, can be observed. Significantly smaller pores are also represented on the surface, however it is difficult to determine their exact size based on SEM imaging. This is due to the blurred image induced by strong electrification of the Aerosil particles and their vibration. The porous structure of PC/Ae results from the granular structure of this composite. Large irregular particles of deposit formed by clumped smaller oval lumps can observed. The inbetween formed pores provide channels for the penetration of water and nitroaromatic molecules into the surface layer and further penetration by capillary forces.

Figure 4

In Supplementary Information in section 5. Scanning Electron Microscopy the individual component images of Figure 4 are presented separately, as Figures S8, S9, ang S10.

3.6. Differential scanning calorimetry

The obtained DSC thermograms are summarized in Figure 5. In the DSC curve recorded for the initial polycarbonate sample, the glass transition at 148 °C can be observed most clearly. It should be remembered that the investigated PC sample contains amorphous thermoplastic polycarbonate originating from molded sheets. The location of the transition and its effect are in agreement with literature data ³⁷. Two endothermic peaks with maximum at 143 °C and 208 °C were recorded on the DSC curve of the sample obtained by evaporating the PC solution in THF. They correspond to the PC melting process, the first one relates to the melting and crystallization of the polymer fraction crystallized from the solution ³⁸, while the second transition corresponds to the melting of the fraction formed by recrystallization of the molten fraction at a low temperature transition, i.e. at 143 °C ³⁹. The enthalpy of the first process is significantly lower than the other one, as the endothermic melting process is

superimposed with the exothermic crystallization process. In the DSC curves for PC/Si aright Article Online PC/Ae, the melting effects of polycarbonate are not as pronounced as in the THF-evaporated sample. In the PC/Si curve, quite small endothermic transitions at 160 °C and 218 °C can be observed, while a clear transition is seen for the PC/Ae sample at 223 °C. The large endothermic peak visible for PC/Si in the 0-140 °C range and the maximum at 75 °C reflects the evaporation of water from the silica pores.

Figure 5

The above discussion of thermograms leads to concluding on the low content of crystalline phase formed in PC/Si and PC/Ae samples after THF evaporation. The presence of solid filler hinders the initial crystallization of PC. The sample recrystallizes only after heating (vide supra), whilst a melting process is observed at higher temperatures. This process is observable only for the PC/Ae sample. The more effortless recrystallization of this sample can be explained primarily by the nanometric particle size of Aerosil, i.e. an average primary particle size of 16 nm, which does not interfere with the formation of crystal lamellae such as the crystalline nanofibers.

3.7. Adsorption on beds

3.7.1. Laboratory scale - 1 l

Experimental setup was established for TNT and then repeated for other nitroaromatics. First, the mixing intensity was determined. It was observed that the system utilizing a mixing rate of 200 rpm involved floating of all the pieces of the bed in the mixed phase. With an increased mixing rate, gradually the solution became cloudy, indicating separation of the bed from the cotton surface. Subsequent experiments were conducted to determine if desalting the solution affected the rate of removal of TNT from the solution. For both 1% wt. and 5% wt. NaCl, no increase in TNT adsorption on the bed was observed. Higher NaCl concentration were not

used in the starting solutions due to the noticeable drop in TNT concentration, probably directorics on the starting solutions due to the noticeable drop in TNT concentration, probably directorics on the starting solutions due to the noticeable drop in TNT concentration, probably directorics of the starting solutions due to the noticeable drop in TNT concentration, probably directorics of the starting solutions due to the noticeable drop in TNT concentration, probably directorics of the starting solutions due to the noticeable drop in TNT concentration, probably directorics of the starting solutions due to the noticeable drop in TNT concentration, probably directorics of the starting solutions due to the noticeable drop in TNT concentration, probably directorics of the starting solutions due to the starti

its precipitation (unpublished data). Hence, further experiments were performed at 200 rpm without using desalting process.

Figure 6 shows TNT adsorption run for up to 50 hours on PC/Ae/C and PC/Si/C bed. The same Figure also shows the adsorption of TNT on a bed containing only PC, as well as adsorption concentration change over time for a TNT solution where 1.5 g of silica was added. No experiment was performed for hydrophobic Aerosil, which could not be dispersed in water. The comparison leads to the first conclusion i.e. poor adsorption of TNT on the PC/C bed and a tiny loss of TNT for the silica suspension. Figure 6 can be used to estimate that these effects constitute about 10% of the adsorbed amount of TNT observed for the PC/Ae/C bed. Furthermore it can be observed that the adsorbed amount of TNT on PC/Si/C bed is significantly lower than in the case of PC/Ae/C bed. For example, after 24 hours of experiment, the amount of adsorbed TNT was about 3 mg/g, while for PC/Ae/C it was over 12 mg/g. Therefore, only PC/Ae/C bed was used further in adsorption studies.

Figure 6

the non-linear model fitting of the PSO equation using the obtained k_2 and q_e values (Table 3). The analysis of curves leads to the conclusion that an adsorption equilibrium state is reached for all analytes after 24 hours of running the process. The highest adsorbed amount was obtained at this point for TNT and 2-NT, whereas the lowest one for nitronaphthalenes. At the initial stage, the curves run shows that the most rapid increase in adsorption is observed for 2-NT and TNT whereas the poorest increase for 1,8-DNT. In consideration to the variations in the concentrations of explosives in solutions during the 1 L scale experiments, it was

determined that by using the PC/Ae/C bed, 94% of the amount of TNT, 89% of 2-NT and

Figure 6 also includes the results for other substances. The curves depicted therein represent

nearly 75% of 2,4-DNT were removed from solution. In the case of nitrotoluenes $_{\text{DOI: }10.1039/\text{D5EW00669D}}$ approximately 60% of the amount was removed.

Based on the R^2 values summarized in Table 3, it is evident that the adsorption process of nitroaromatics on the PC/Ae/C bed is less consistent with the pseudo-first-order (PFO) kinetic model compared to the pseudo-second-order (PSO) model. In the case of PSO equation, R^2 values exceed 0.99 for all compounds. Figure S12 in the Supplementary Information presents the fittings of the applied kinetic models in the form of linear equations to the obtained experimental data. For the PSO model, an excellent fit of the data to the linear equation can be observed, which is consistent with the high R^2 values. Good fitting to the PSO kinetic model suggests that, in addition to the diffusion of nitroaromatic molecules to the surface of the sorbent bed, the adsorption rate may also be influenced by intraparticle diffusion as well as the occurrence of π - π interactions between the π -acceptor (nitroaromatics) and the π -donor (polycarbonate surface). For such interactions to occur, a proper spatial orientation of the donor and acceptor molecules is required 40 . A comparison of determined q_e equilibrium adsorption values and experimentally determined q values (Table 3) shows that q_e values calculated from the PSO equation are comparable with experimental equilibrium data. The maximum difference between q_e and q is 0.45 mg/g.

As shown in Table 3, the k_1 values obtained from the PFO model are relatively consistent $(0.017\text{--}0.019~\text{min}^{-1})$, whereas the k_2 values derived from the PSO model differ considerably $(0.00067\text{--}0.00123~\text{g mg}^{-1}~\text{min}^{-1})$. These discrepancies in k_2 appear to correlate with the molecular structure of the adsorbates. The highest k_2 values were observed for nitro compounds containing a single nitro group (2-NT and 1-NN), while the lowest values were recorded for compounds with three nitro groups (2,4,6--TNT and 1,3,5--TNB). This suggests that the k_2 constant, which reflects the rate of adsorption (i.e., the binding or settling of adsorbate molecules onto the adsorbent surface), may in this case be influenced by the

molecular geometry and the accessibility of adsorption sites, potentially governed by $\pi_1\pi_1\pi_3$ view Article Online $\pi_1\pi_2\pi_3$ interactions (vide supra).

475 Table 3

476

477

478

479

480

481

482

483

484

485

486

487

491

492

493

494

495

496

3.7.2. Laboratory scale – adsorption isotherms

The results presented in Table 4 summarizes the constants calculated from the linearized forms of the Langmuir and Freundlich models, as well as the corresponding R^2 values. Higher R^2 values were obtained for the Freundlich model. Figure 7 presents the experimental adsorption data obtained at the aforementioned three temperatures, along with curves representing the nonlinear Langmuir and Freundlich isotherm models 31 , plotted using the calculated constants Q_m and K_L , as well as n and K_F . As can be seen in Figure 8, the curves representing the Freundlich isotherms show a very good fit to the experimental data over the entire range of equilibrium concentrations, while the Langmuir isotherms show only an acceptable fit at low concentrations. Therefore, it can be concluded that TNT adsorption in the studied system follows the Freundlich model and is based on multilayer adsorption on a heterogeneous surface.

488 Table 4

489 Figure 7

490 3.7.3. Laboratory scale – adsorption thermodynamics

The ΔG values presented in Table 5 are negative at all investigated temperatures, confirming that the adsorption of TNT onto the PC/Ae/C is spontaneous and thermodynamically favourable. The observed negative ΔH values indicate that the process is exothermic, with its intensity decreasing as the temperature increases. The ΔH values are greater than – 40 kJ mol⁻¹, suggesting a physisorption mechanism ⁴¹. The negative ΔS values indicate decreased randomness at the solid–liquid interface, likely resulting from the ordered adsorption of TNT

on sorption sites via π -donor (e.g., carbonyl groups or oxygen atoms in the C–O–C bonds of Article Online polycarbonate) to π -acceptor (electron-deficient aromatic ring of TNT) interactions. Furthermore, data from Table 5 suggest that the entropic contribution to the Gibbs free energy change is minimal, increasing it by approximately 4 kJ mol⁻¹. Therefore, TNT adsorption onto the PC/Ae/C composite is enthalpy - driven, involving relatively strong interactions with the surface. In conclusion, it is worth mentioning that the use of incorrect K_{eq} values in Equations 6 and 7 may, for example, lead to inconsistencies in the calculated values of ΔS^{42} . Table 5 presents the value of ΔS calculated based on K_L expressed in L/g. This value is over ten times lower than the correctly calculated ΔS based on the dimensionless constant K_L^0 .

Table 5

3.7.4. Laboratory scale - real surface water

Last column of Table 3 represents the collation of q_{river} adsorption values of nitroaromatic substances in the river water, obtained in experimental 1 L scale setup. It can be seen that q and q_{river} values are quite similar, and the differences between them are random, ranging from -1.19 to 0.90 mg / g. To determine whether the type of water affects the adsorption capacity on the PC/Ae/C bed, the average adsorption value was calculated from the results for six tested substances for each type of water. Then, using the t-test 50 , it was examined whether these average values differ statistically from each other. The test showed that there are no statistically significant differences at the 0.05 significance level between the obtained results – the mean experimental equilibrium adsorption values for nitroaromatics in river water and redistilled water. The calculated t value for data from Table 3 is |t| = 0.176. At a significance level 0.05 and 10 degrees of freedom (6 + 6 - 2) the critical value is t = 2.228. The calculated t is less than critical t value so the null hypothesis is retained: there is no evidence that the average equilibrium adsorption values for nitroaromatics in river water and redistilled water differs from each other. In conclusion, it can be assumed that the PC/Ae/C adsorbent is

suitable for removing explosive substances from the real water sample, as used in the View Article Online on the experiment. Most likely, river water dissolved components are not adequately adsorbed on the PC/Ae/C surface.

To confirm this hypothesis, primarily concerning dissolved organic matter (DOM),

measurements were carried out using UV-Vis spectroscopy in the range of 200–800 nm. UV-Vis absorption is commonly used to provide information on dissolved organic matter (DOM) in aqueous systems ⁵¹. The study was conducted on the original river water sample, on the same water after an experiment in a 1-liter scale with the PC/Ae/C composite (mass of the adsorptive phase ca. 36 grams, see point 2. Materials and methods), and on the water after a 1-liter scale experiment using Norit SX-2 activated carbon (mass of the adsorbent 36 grams). The results presented in Figure S11 (Supplementary Information) show that the UV spectra of the original sample and the sample after adsorption on the PC/Ae/C are nearly identical. It can only be concluded that absorbance in the 230–280 nm range is slightly reduced. In contrast, after adsorption on the activated carbon, a significant decrease in absorbance within this range was observed. Therefore, the conclusion regarding the weak adsorption of DOM on the PC/Ae/C composite seems to be confirmed. Strong adsorption of DOM on activated carbons has been reported in numerous studies ⁵² ⁵³. The adsorption of soluble natural components causes a serious problem when using activated carbons to remove harmful pharmaceutical ingredients ⁵⁴, perfluorinated compounds ⁵⁵, or methylene blue dye ⁵⁵ from surface water.

3.7.5. Bench scale - 16 l

Figure 8 presents the results of kinetic experiments conducted at a 16 L scale for four nitroaromatic compounds. Similar to Figure 6, which shows data for the 1 L scale, the curves represent a non-linear fit of the PSO model to the experimental data. Analysis of Figure 8 indicates that the adsorption equilibrium state is reached for all analytes after 24–28 hours of process operation. The highest adsorbed amounts at this stage of the experiment were

548

549

550

551

552

553

554

555

556

557

558

559

560

561

562

563

564

565

566

567

568

569

Open Access Article. Published on 29 July 2025. Downloaded on 8/11/2025 11:18:36 AM.

This article is licensed under a Creative Commons Attribution 3.0 Unported Licence.

observed for TNT and 2-NT, while the lowest was recorded for TNB. At the initial stage of warticle Online O the process, the shape of the curves suggests that the most rapid increase in adsorption occurs for 2-NT, whereas the slowest increase is observed for TNB. The lower part of Table 3 summarizes the parameter values calculated for the applied kinetic models, PFO and PSO, for the bench-scale. The linear fits of these kinetic models to the experimental data are shown in Figure S13 in the Supporting Information (SI). Based on the highest R² values and the excellent agreement of the fitted lines with the experimental data, it is evident that the adsorption process of nitroaromatics at the 16 L scale, similarly to the 1 L scale, follows the PSO kinetic model. The good fit to the PSO model indicates that the adsorption process at both scales proceeds similarly, despite the completely different experimental setups, i.e. hydrodynamic conditions and mass transfer mechanism. Thus, in the 16 L setup, the nitroaromatic solution circulated through a glass column containing loosely packed, stationary bed fragments (1×1 cm), whereas in the 1 L setup, solution and bed mixing was carried out using a mechanical stirrer. The adsorbent mass in the 16 L system was proportionally scaled up, i.e. sixteen times greater, while the analytes concentration remained the same (25 mg/L). The q_e values for the larger scale were approximately 0.9 to 1.9 mg/g lower, but overall, they can be considered comparable to those obtained at the 1 L scale. As observed for the 1 L scale, in the 16 L setup, the highest k_2 values was recorded for nitro compound containing one nitro group (2-NT), whereas the lowest k₂ values were obtained for compounds with three nitro groups in their molecules, namely TNT and TNB.

Figure 8

570

572

573

574

575

576

577

578

579

580

581

582

583

584

585

586

587

588

589

590

591

592

593

3.7.6. Solvent desorption studies. Cost-effectiveness analysis of the process in an industrial context. View Article Online DOI: 10.1039/D5EW00669D

The possibility of desorbing TNT adsorbed on the PC/Ae/C bed was investigated during experiments conducted using acetonitrile (ACN). Using acetonitrile under the conditions described above, it was possible to wash out 64% ($\pm 12\%$) of the substance. It is worth mentioning that this experiment was performed using ACN under preliminarily selected, nonoptimized conditions and was carried out solely to assess the efficiency of the desorption. For the synthesized PC/Ae/C adsorbent, the material cost is primarily associated with Aerosil, priced at approximately €5 per kilogram. The other constituents: cotton, polycarbonate, and tetrahydrofuran are waste derived materials, for which market valuation is either negligible or indeterminate, especially since both waste collection and disposal incur costs. According to the procedure detailed in the Experimental section, the incorporation of 1 kg of Aerosil yields approximately 5 m² of adsorbent bed. In the desorption method outlined in the current section, ACN was utilized at a volume of 1 mL per cm² of adsorbent surface area. Accordingly, the desorption of a 5 m² bed would require 50 L of ACN. The cost of 1 L technical-grade ACN in the domestic market is approximately €10, resulting in a total solvent cost of €500. In comparison, the use of technical-grade acetone would reduce the total cost to approximately €100. Nevertheless, from a purely economic standpoint, solvent-based desorption remains financially unjustifiable. The authors propose that the most economically viable and environmentally responsible method for the disposal of the used adsorbent beds is incineration. The presence of energetic compounds in a finely dispersed and phlegmatized form significantly mitigates the risk of detonation. Moreover, the explosives content in the deposit is at the level of 10 mg per gram

(1% by weight), therefore a self-sustaining combustion reaction cannot occur ⁴³. It is also

595

596

597

598

599

600

601

602

603

604

605

606

607

608

609

610

611

612

613

614

615

616

noteworthy that cotton- or cellulose-based medical wastes are commonly disposed of via View Article Online Online

The reported average carbon footprints (GWP) for the materials used are as follows: cotton 1

3.7.7. Estimation of the carbon footprint (GWP) for the PC/Ae/C adsorbent

kg CO₂-eq/kg ⁴⁴, polycarbonate 5 kg CO₂-eq/kg ⁴⁵, and Aerosil average 1 kg CO₂-eq/kg ⁴⁶. The average GWP of the prepared composite (produced from new, non-recycled materials) is 2.4 kg CO₂-eq/kg. This was calculated based on the composition of the sorbent described in the paper: 35 wt.% polycarbonate, 35 wt.% Aerosil, and 30 wt.% cotton. It should be noted, however, that extending the lifespan of products and promoting their reuse can significantly reduce their carbon footprint. For instance, for PET (a polymer containing chemical groups similar to those in polycarbonate), recycling can reduce the GWP by a factor of four ⁴⁷, while for cotton, the reduction can reach 25% 48. The data for PET was used because no data for recycled polycarbonate could be found. Calculations based on these reductions yield an average GWP of approximately 1.0 kg CO₂-eg/kg for the prepared adsorbent. When comparing the sorption capacities for TNT on the adsorbents listed in Table 6, it becomes evident that GAC (granular activated carbon) has a capacity about seven times higher than that of the PC/Ae/C sorbent. Therefore, assuming that seven times more of the PC/Ae/C composite would be required to achieve the same TNT removal efficiency, the total GWP for 7 kg of this sorbent would amount to 7 kg CO₂-eq (recycled components) and 16 kg CO₂-eq (non-recycled components). At the same time the mean GWP reported in the literature for GAC is 11 kg CO₂-eq/kg ⁴⁹. Taking into account the energy and chemicals required for the production and regeneration of GAC, the PC/Ae/C sorbent prepared from recycled components appears to have considerable

potential - especially since it can be incinerated after use (3.7.4) with only a little mineral View Article Online Solid residue, and provide energy for other processes in waste treatment plants.

4. Conclusions

617

618

619

620

621

622

623

624

625

626

627

628

629

630

631

632

633

634

635

636

637

638

639

640

The study demonstrated the effectiveness of a new material obtained in accordance with the principles of sustainable development and a circular economy, for the removal of nitroaromatic explosives from water. The prepared material contained ca. 30% cotton, 35% polycarbonate and 35% fumed silica – Aerosil. While preparing the material, i.e. the fabric coated with adsorbent – the minimum environmental impact had to be ensured, i.e. (i) the material was obtained from waste cotton and polycarbonate raw materials, (ii) the used silica and tetrahydrofuran (a waste solvent from chromatography) are environmentally harmless, (iii) the preparation process consumed little energy, nor chemical reactions were used, (iv) the application of prepared bed required the use of simple equipment and processing techniques, easily scalable to larger-scale processes. The sorption capacities presented in this work for nitroaromatics (8–12 mg/g) are lower than those reported for more effective adsorbents, such as activated carbons, shown in Table 6. However, they can be regarded as a promising results, especially when the significant drawbacks of other adsorbents are taken into account. For instance, the production of activated carbon, regardless of the precursor, requires chemicals, is energy-intensive and associated with significant emissions of gases such as CO₂, CO, H₂S, and hydrocarbons, while the synthesis of specialized polymers (Table 6) is time-consuming and often generates

toxic waste. A major advantage of the obtained PC/Ae/C bed is usage of waste materials and

also its relatively simple disposal through incineration, especially since, as previously shown,

solvent desorption methods are economically unviable. The obtained results provide

foundation for further development of the proposed sorption material as well as the

27

Open Access Article. Published on 29 July 2025. Downloaded on 8/11/2025 11:18:36 AM.

(cc) BY

This article is licensed under a Creative Commons Attribution 3.0 Unported Licence.

the sorption column or the application of a series of smaller columns can be considered as well. In relation to the preparation process, primarily in terms of cost reduction and smaller environmental impact, Aerosil can be effectively replaced with other components such as natural aluminosilicates or recycled components such as fly ash.

Credit authorship contribution statement

Waldemar Tomaszewski: Conceptualization, Investigation (Lab scale, FTIR, HPLC), Formal analysis, Writing - original draft, Writing - review & editing. Andrzej Krasiński:

Conceptualization, Investigation (Bench scale), Formal analysis, Writing - review & editing.

Magdalena Zybert: Investigation (nitrogen adsorption). Piotr Wieciński: Investigation (SEM).

Tomasz Gołofit: Investigation (DSC).

Declaration of Competing Interest

The authors declare that they have no known competing financial interests or personal relationships that could have appeared to influence the work reported in this paper.

Acknowledgments

Authors would like to thank prof. Grażyna Zofia Żukowska for her help with the Raman analysis.

This work was supported by Warsaw University of Technology under I-Chem.4 project of the Scientific Council for Chemical Engineering.

663 References View Article Online
DOI: 10.1039/D5EW00669D

664	1	Mat	erial	s Mar	ket Rep	ort 2023	- Te	extile	e Excl	nange) ,
		4	11.		4	/1		4		,	

- https://textileexchange.org/knowledge-center/reports/materials-market-report-2023/,
- 666 (accessed 21 October 2024).
- Plastics Europe launches Plastics the fast Facts 2023 Plastics Europe,
- https://plasticseurope.org/media/plastics-europe-launches-the-plastics-the-fast-facts-
- 669 2023/, (accessed 21 October 2024).
- 670 3 M. Tripathi, M. Sharma, S. Bala, V. K. Thakur, A. Singh, K. Dashora, P. Hart and V.
- 671 K. Gupta, Curr. Res. Biotechnol., 2024, 7, 100225.
- 672 4 M. Y. Khalid, Z. U. Arif, W. Ahmed and H. Arshad, Sustain. Mater. Technol., 2022,
- **31**, e00382.
- 674 5 R. M. Abdelhameed, M. El-Zawahry and H. E. Emam, *Polymer (Guildf).*, 2018, **155**,
- 675 225–234.
- 676 Y.-J. L. Mi-Kyung Kim, Seok-Han Yoon, Tae-Kyeong Kim, *J. Korean Soc. Dye.*
- 677 Finish., 2005, 17, 20–29.
- 678 7 D. Tian, X. Zhang, C. Lu, G. Yuan, W. Zhang and Z. Zhou, *Cellulose*, 2014, **21**, 473–
- 679 484.
- 680 8 M. MAHMOUD NASEF, H. SAIDI, Z. UJANG and K. Z. MOHD DAHLAN, J. Chil.
- 681 *Chem. Soc.*, 2010, **55**, 421–427.
- 682 9 J. Saleem, M. Adil Riaz and M. Gordon, J. Hazard. Mater., 2018, **341**, 424–437.
- 683 10 N. A. El Essawy, S. M. Ali, H. A. Farag, A. H. Konsowa, M. Elnouby and H. A.
- 684 Hamad, *Ecotoxicol. Environ. Saf.*, 2017, **145**, 57–68.

This article is licensed under a Creative Commons Attribution 3.0 Unported Licence.

Open Access Article. Published on 29 July 2025. Downloaded on 8/11/2025 11:18:36 AM.

685 11 B. Hoek, Med. Confl. Surviv., 2004, **20**, 326–333.

- View Article Online DOI: 10.1039/D5EW00669D
- 686 12 J. C. Pennington and J. M. Brannon, *Thermochim. Acta*, 2002, **384**, 163–172.
- 687 13 R. A. Young, in *Encyclopedia of Toxicology*, Elsevier, 2014, pp. 179–182.
- 688 14 GUIDE TO EXPLOSIVE ORDNANCE POLLUTION OF THE ENVIRONMENT -
- GICHD, https://www.gichd.org/publications-resources/publications/guide-to-
- explosive-ordnance-pollution-of-the-environment-1/, (accessed 22 October 2024).
- 691 15 J. D. Rodgers and N. J. Bunce, *Water Res.*, 2001, **35**, 2101–2111.
- 692 16 S. Olavi Pehkonen, S. Zou, Y.-T. Hung, J. Paul Chen and L. Wang, in *Handbook of*
- Industrial and Hazardous Wastes Treatment, CRC Press, 2004, pp. 1113–1124.
- 694 17 G. Yardin and S. Chiron, *Chemosphere*, 2006, **62**, 1395–1402.
- P. P. Kanekar, S. S. Sarnaik, P. S. Dautpure, V. P. Patil and S. P. Kanekar, 2014, pp.
- 696 67–86.
- 697 19 K. Panz and K. Miksch, J. Environ. Manage., 2012, 113, 85–92.
- 698 20 J. T. Walsh, R. C. Chalk and C. Merritt, *Anal. Chem.*, 1973, **45**, 1215–1220.
- 699 21 H. M. Heilmann, U. Wiesmann and M. K. Stenstrom, Environ. Sci. Technol., 1996, 30,
- 700 1485–1492.
- 701 22 P. C. Ho and C. S. Daw, *Environ. Sci. Technol.*, 1988, **22**, 919–924.
- 702 23 K. Misra, S. K. Kapoor and R. C. Bansal, *J. Environ. Monit.*, 2002, 4, 462–464.
- 703 24 B. Charmas, M. Zięzio, W. Tomaszewski and K. Kucio, Colloids Surfaces A
- 704 *Physicochem. Eng. Asp.*, 2022, **645**, 128889.
- 705 25 G. L. McEneff, B. Murphy, T. Webb, D. Wood, R. Irlam, J. Mills, D. Green and L. P.

- W. Tomaszewski, V. M. Gun'ko and J. Skubiszewska-Zięba, J. Sep. Sci., 2016, 39, 707 26
- 708 1524-1532.
- E. C. L. Mohammad Hadi Dehghani, Shabnam Ahmadi, Soumya Ghosh, Amina 709 27
- Othmani, Christian Osagie, Maryam Meskini, Samar Sami AlKafaas, Alhadji 710
- Malloum, Waheed Ahmad Khanday, Ajala Oluwaseun Jacob, Ömür Gökkuş, Andrew 711
- 712 Oroke, Obialor Martins Chineme, Rama Rao Karri, Arab. J. Chem., 2023, 16, 105303.
- M. V. Galaburda, V. M. Bogatyrov, W. Tomaszewski, O. I. Oranska, M. V. 713 28
- 714 Borysenko, J. Skubiszewska-Zieba and V. M. Gun'ko, Colloids Surfaces A
- Physicochem. Eng. Asp., 2017, **529**, 950–958. 715
- 716 29 G. Crini, H. N. Peindy, F. Gimbert and C. Robert, Sep. Purif. Technol., 2007, 53, 97-
- 110. 717

This article is licensed under a Creative Commons Attribution 3.0 Unported Licence.

Open Access Article. Published on 29 July 2025. Downloaded on 8/11/2025 11:18:36 AM.

- Y. S. Ho and G. McKay, *Process Biochem.*, 1999, **34**, 451–465. 718 30
- 719 K. Y. Foo and B. H. Hameed, *Chem. Eng. J.*, 2010, **156**, 2–10. 31
- P. S. Ghosal and A. K. Gupta, J. Mol. Liq., 2017, 225, 137–146. 720 32
- J. Dybal, P. Schmidt, J. Baldrian and J. Kratochvíl, *Macromolecules*, 1998, **31**, 6611– 721 33
- 722 6619.
- 723 H. Uematsu, N. Higashitani, A. Yamaguchi, A. Fukuishima, T. Asano, S. Mitsudo, S. 34
- Sugihara, M. Yamane, T. Irisawa, Y. Ozaki and S. Tanoue, Surfaces and Interfaces, 724
- 2022, 34, 102300. 725
- M. Thommes, K. Kaneko, A. V. Neimark, J. P. Olivier, F. Rodriguez-Reinoso, J. 726 35
- Rouguerol and K. S. W. Sing, *Pure Appl. Chem.*, 2015, **87**, 1051–1069. 727

Open Access Article. Published on 29 July 2025. Downloaded on 8/11/2025 11:18:36 AM.

This article is licensed under a Creative Commons Attribution 3.0 Unported Licence.

- 728 36 Y. Xu, Y. Gao, X. Wang, J. Jiang, J. Hou and Q. Li, *Macromol. Mater. Eng* View Article Online Online Online
- 729 DOI:10.1002/mame.201700054.
- 730 37 R. F. Boyer, J. Macromol. Sci. Part B, 1973, 7, 487–501.
- 731 38 H. Schorn, M. Heß and R. Kosfeld, in *Integration of Fundamental Polymer Science*
- 732 and Technology—2, Springer Netherlands, Dordrecht, 1988, pp. 385–388.
- 733 39 S. Sohn, A. Alizadeh and H. Marand, *Polymer (Guildf)*., 2000, **41**, 8879–8886.
- 734 40 R. Thakuria, N. K. Nath and B. K. Saha, *Cryst. Growth Des.*, 2019, **19**, 523–528.
- 735 41 V. J. Inglezakis and A. A. Zorpas, *Desalin. Water Treat.*, 2012, **39**, 149–157.
- 736 42 H. N. Tran, Adsorpt. Sci. Technol., DOI:10.1155/2022/5553212.
- 737 43 The European Standard EN 1127-1:2007, Explosive atmospheres Explosion
- 738 prevention and protection Part 1: Basic concepts and methodology, European
- 739 *Committee For Standardization 2007, Brussels*, .
- 740 44 S. S. Madhuri Nigam, Prasad Mandade, Bhawana Chanana, *Int. Arch. Appl. Sci.*
- 741 *Technol.*, 2016, 7, 06–12.
- 742 45 M. F. Ashby, Materials and the Environment: Eco-informed Material Choice,
- 743 Butterworth-Heinemann is an imprint of Elsevier, Ashby, M. F. (2021). Materials and
- the Environment: Eco-informed Material Choice. In Materials and the Environment:
- 745 Eco-informed Material Choice (Third). Butterworth-Heinemann is an imprint of
- 746 Elsevier. https://doi.org/10.1016/B978-0-12-821521-0.01001-X, 3rd ed., 2021.
- 747 46 https://hpqsilicon.com/wp-
- content/uploads/2024/08/HPQ DECK AUGUST 29 2024 V1.pdf.
- 749 E. W. Gabisa, C. Ratanatamskul and S. H. Gheewala, Sustainability, 2023, 15, 11529.

- 750 48 S. Roy, Y. Y. J. Chu and S. S. Chopra, *Resour. Conserv. Recycl. Adv.*, 2023 19 View Article Online Online
- 751 200177.
- 752 49 P. Bayer, E. Heuer, U. Karl and M. Finkel, Water Res., 2005, 39, 1719–1728.
- 753 50 M. H. Herzog, G. Francis and A. Clarke, in *Understanding Statistics and Experimental*
- 754 Design . Learning Materials in Biosciences, Springer, Cham., 2019, pp. 51–59.
- 755 51 E. C. Minor, M. M. Swenson, B. M. Mattson and A. R. Oyler, *Environ. Sci. Process.*
- 756 *Impacts*, 2014, **16**, 2064–2079.
- 757 52 T. Karanfil, M. Kitis, J. E. Kilduff and A. Wigton, Environ. Sci. Technol., 1999, 33,
- **758** 3225–3233.
- 759 53 B. Schreiber, T. Brinkmann, V. Schmalz and E. Worch, Water Res., 2005, 39, 3449–
- 760 3456.
- 761 54 L. F. Delgado, P. Charles, K. Glucina and C. Morlay, Sep. Sci. Technol., 2015, 50,
- 762 1487–1496.
- 763 55 J. Yu and J. Hu, *J. Environ. Eng.*, 2011, **137**, 945–951.
- 764 56 V. Marinović, M. Ristić and M. Dostanić, *J. Hazard. Mater.*, 2005, **117**, 121–128.
- 765 57 J.-W. Lee, T.-H. Yang, W.-G. Shim, T.-O. Kwon and I.-S. Moon, J. Hazard. Mater.,
- 766 2007, **141**, 185–192.
- 767 58 F. An, X. Feng and B. Gao, *J. Hazard. Mater.*, 2009, **168**, 352–357.
- 768 59 Y. Xu, H. Zhu, S. Mo, Y. Mao, C. Zhong, Y. Huang, R. Yuan, M. Zheng, M. Zhou and
- 769 G. Chang, *Polymer (Guildf).*, 2024, **300**, 126993.
- 770 60 Y. Liu, S. Zeng, X. He, Y. Wu, Y. Liu and Y. Wang, *Molecules*, 2024, **29**, 5822.
- 771 61 X.-E. Shen, X.-Q. Shan, D.-M. Dong, X.-Y. Hua and G. Owens, *J. Colloid Interface*

Open Access Article. Published on 29 July 2025. Downloaded on 8/11/2025 11:18:36 AM.

This article is licensed under a Creative Commons Attribution 3.0 Unported Licence.

772 *Sci.*, 2009, **330**, 1–8.

View Article Online DOI: 10.1039/D5EW00669D

773

774 TABLES

Table 1. The intensity ratio of the bands representing ordered (727 cm⁻¹, 1248 cm⁻¹) and disordered (735 cm⁻¹, 1235 cm⁻¹) states of the adsorbents, obtained by the deconvolution of samples Raman spectra.

G 1	Intensity ratio	Intensity ratio
Sample	I_{727}/I_{735}	I_{1248}/I_{1235}
initial PC	0.32	1.03
PC/cotton	0.84	1.05
PC/ silica/cotton/	1.20	1.17
PC/Aerosil/cotton	1.24	1.26

778

779 Table 2. Physicochemical properties of the studied materials

Sample	Description	S_{BET} (m ² g ⁻¹) ¹	V_p (cm ³ g ⁻¹) ²	d _{av} (nm) ³
a	cotton	0.7	< 0.01	9.6
b	cotton + polycarbonate	0.6	< 0.01	13.0
c	cotton + polycarbonate + Aerosil R972V	24.6	0.14	23.0
d	cotton + polycarbonate + silica	72.9	0.12	6.6

⁷⁸⁰ $\frac{1}{1}$ S_{BET} – specific surface area determined based on the BET adsorption model.

783

⁷⁸¹ 2 V_p – total pore volume determined based on the BJH adsorption model.

⁷⁸² 3 d_{av} – average pore diameter

Table 3. Kinetic parameters for adsorption of nitroaromatics on PC/Ae/C. Experiments in the article Online
 laboratory scale - 1 L and bench scale - 16 L.

	q mg/g	Pseudo-first order			Pseudo-second order			River water 48 h
Substance		q _e mg/g	k ₁	\mathbb{R}^2	q _e mg/g	k ₂ g/ (mg min)	R ²	q _{river} mg/g
				Laborat	ory scale	e 1 L		
2,4,6- TNT	11.20	7.67	0.00193	0.962	11.65	0.00067	0.999	12.10
2,4-DNT	10.10	8.08	0.00180	0.959	10.30	0.00076	0.997	10.80
2-NT	10.66	5.16	0.00174	0.908	10.96	0.00116	0.999	9.85
1,3,5- TNB	9.49	7.16	0.00184	0.979	9.81	0.00073	0.998	8.30
1-NN	8.20	4.95	0.00182	0.929	8.41	0.00123	0.999	9.10
1,8-DNN	7.65	5.33	0.00174	0.956	7.94	0.00092	0.998	8.05
			Bench scal	le 16 L				
2,4,6- TNT	9.15	7.83	0.00342	0.958	10.06	0.00063	0.999	
2,4-DNT	8.36	7.36	0.00351	0.960	9.20	0.00066	0.997	
2-NT	8.80	4.05	0.00358	0.857	9.05	0.00176	0.999	
1,3,5- TNB	8.16	7.08	0.00303	0.964	8.91	0.00065	0.997	

786 q – experimental equilibrium adsorption

 q_e – calculated equilibrium adsorption

This article is licensed under a Creative Commons Attribution 3.0 Unported Licence.

Open Access Article. Published on 29 July 2025. Downloaded on 8/11/2025 11:18:36 AM.

788 k_1 – rate constant of the PFO kinetic equation

789 k_2 – rate constant of the PSO kinetic equation

 R^2 – coefficient of determination

791 q_{river} – experimental equilibrium adsorption for river water

Open Access Article. Published on 29 July 2025. Downloaded on 8/11/2025 11:18:36 AM.

This article is licensed under a Creative Commons Attribution 3.0 Unported Licence.

Table 4. Adsorption of TNT on PC/Ae/C bed. Parameters for Langmuir and Freundlich View Article Online
 isotherm models.

I	Langmuir model		F	Freundlich model				
26 °C / 299 K								
Q _m (mg/g)	K _L (L/mg)	R ²	n	K _F (L/mg)	R ²			
3.08 ± 0.21	5.05 ± 0.22	0.97	1.54 ± 0.15	3.98 ± 0.12	0.99			
36 °C / 309 K								
3.37 ± 0.19	2.97 ± 0.20	0.98	1.49 ± 0.18	3.14 ± 0.16	0.99			
46 °C / 319 K								
3.21 ± 0.18	1.94 ± 0.11	0.98	1.43 ± 0.14	2.36 ± 0.15	0.99			

794 $q_m - maximum$ adsorption capacity

795 K_L – Langmuir constant

 $796 \qquad n-constant$

797 K_F – Freundlich constant

 R^2 – coefficient of determination

Table 5. Thermodynamic parameters of TNT adsorption on the PC/Ae/C bed calculated based on the Langmuir equilibrium constant K_L and the dimensionless Langmuir equilibrium constant K_L⁰.

Temperature [K]	$K_L^0[]$	$K_{L}[L/g]$	ΔH [kJ/mol]	ΔS [J/mol K]	ΔG° [kJ/mol]
299	1147306.54				-34.71
309	674326.26		-38.02	-11.17	-34.50
319	440632.20			•	-34.49
299		5.05			-4.03
309	-	2.97	-38.02	-113.72	-2.80
319	-	1.94	•	•	-1.76

803 ΔH – enthalpy change,

804 ΔS – entropy change,

805 ΔG° – Gibbs free energy change.

808

809

810

811

812

813

814

815

816

817

818

819

820

Table 6 Examples of sorption capacities obtained for TNT on different adsorbents.

View Article Online DOI: 10.1039/D5EW00669D

Adsorbent	Method	C ₀ TNT [mg/L]	TNT sorption capacity [mg/g]	Calculation method	Year / Ref.
PC/Ae/C	KE	1 - 25	12	q _e from PSO kinetic model	this work
GAC	CDA	30-170	80	breakthrough curves	2005 / 56
AC	BSE	10-100	10	Langmuir isotherm	2007 / 57
PAM/SiO ₂	CDA	100	0.9	breakthrough curves	2009 / 58
PTIM	BSE	50 - 350	400	Langmuir isotherm	2024 / 59
clip-SOF	d-SPE	1	40	C ₀ and C _R	2024 / 60
MWCNTs	BSE	100 - 400	40 (3-NT)	Langmuir isotherm	2009 / 61

C₀ – initial concentration of TNT

C_R – residual concentration TNT

PC/Ae/C – composite of polycarbonate and Aerosil on cotton

KE – kinetic experiments

GAC – granular activated carbon

AC – activated carbon

CDA – column dynamic adsorption

BSE – batch sorption experiments – shaking

PAM/SiO₂ – polyacrylamide grafted to SiO2

PTIM – indole-based porous organic polymer

clip-SOF – glycoluril-derived molecular-clip-based supramolecular organic framework

d-SPE – dispersive solid phase extraction

MWCNTs - multiwalled carbon nanotubes

3-NT – 3-nitrotoluene.

View Article Online DOI: 10.1039/D5EW00669D

Data availability statement

All data are available in the main manuscript and ESI.

Open Access Article. Published on 29 July 2025. Downloaded on 8/11/2025 11:18:36 AM.

This article is licensed under a Creative Commons Attribution 3.0 Unported Licence.